Copyright Warning & Restrictions

The copyright law of the United States (Title 17, United States Code) governs the making of photocopies or other reproductions of copyrighted material.

Under certain conditions specified in the law, libraries and archives are authorized to furnish a photocopy or other reproduction. One of these specified conditions is that the photocopy or reproduction is not to be "used for any purpose other than private study, scholarship, or research." If a, user makes a request for, or later uses, a photocopy or reproduction for purposes in excess of "fair use" that user may be liable for copyright infringement,

This institution reserves the right to refuse to accept a copying order if, in its judgment, fulfillment of the order would involve violation of copyright law.

Please Note: The author retains the copyright while the New Jersey Institute of Technology reserves the right to distribute this thesis or dissertation

Printing note: If you do not wish to print this page, then select "Pages from: first page # to: last page #" on the print dialog screen

ABSTRACT

THERMAL PROPERTIES OF GRAPHENE

by

Vishal Vijay Nakhate

The two-dimensional (2D) monolayer structure of carbon atoms were initially considered as unstable. The 2D materials have recently been discovered and many researchers have started analyzing these materials. Graphene, a two-dimensional allotrope of graphite with sp2 bonded carbon atoms, is arranged in honeycomb structure. Graphene has excellent thermal conductivity and can be considered as a potential material for applications in the electronics industry where heating of materials is a serious concern.

In this study, thermal properties of p and n doped graphene nanosheets and nanoribbons are studied as function of percentage composition of the dopants and the direction of dissipation of heat flux. Phonon dispersion spectra are presented for these structures using Materials Studio. Non- Equilibrium Molecular Dynamics simulation has been implemented for the calculations.

Structures of doped graphene are modeled using Density Functional Theory to study the phonon dispersion. The specific heat of pristine and doped graphene structures are reported.

THERMAL PROPERTIES OF GRAPHENE

by
Vishal Vijay Nakhate

A Thesis
Submitted to the Faculty of
New Jersey Institute of Technology
in Partial Fulfillment of the Requirements for the Degree of
Master of Science in Materials Science and Engineering

Interdisciplinary Program in Materials Science and Engineering

May 2015

APPROVAL PAGE

THERMAL PROPERTIES OF GRAPHENE

Vishal Vijay Nakhate

Dr. N. M. Ravindra, Thesis Advisor Date
Professor, Department of Physics, NJIT
Director, Interdisciplinary Program in Materials Science & Engineering, NJIT

Dr. Michael Jaffe, Committee Member Date
Research Professor, Department of Biomedical Engineering, NJIT

Dr. Halina Opyrchal, Committee Member Date
Senior University Lecturer, Department of Physics, NJIT

Mr. Balraj. S. Mani, Committee Member Date
University Lecturer, Department of Mechanical & Industrial Engineering, NJIT

Dr. Willis B. Hammond, Committee Member Date
CEO, W. B. Hammond Associates, LLC

BIOGRAPHICAL SKETCH

Author: Vishal Vijay Nakhate

Degree: Master of Science

Date: May 2015

Undergraduate and Graduate Education:

- Master of Science in Materials Science and Engineering, New Jersey Institute of Technology, Newark, NJ, 2015

- Bachelor of Technology in Metallurgical Engineering, College of Engineering, Pune, Maharashtra, India, 2012

Major: Materials Science and Engineering

I would like to dedicate this work to

my Parents, Dr.Vijay S. Nakhate and Mrs. Vaishali V. Nakhate;

my family, Vikrant V. Nakhate, Viren V. Nakhate;

and Sinha family, Mr. Anil Sinha, Mrs. Rekha Sinha, Anjana Sinha, Anshu Sinha;

for their continuous support and motivation!

ACKNOWLEDGEMENTS

I would like to thank with immense gratitude to Dr. N. M. Ravindra, as an advisor, for his continuous support, invaluable insights and inspiration during the entire course of research. His guidance at all times has been of immense value. Without his excellent advice and guidance on this topic, this work could not have been accomplished.

I would like to thank my committee members Dr. Michael Jaffe, Dr. Halina Opyrychal, Mr. Balraj S. Mani, Dr. Willis B. Hammond for serving as members in my committee and providing me with their helpful comments after reading the manuscript thoroughly.

I am thankful to the MTSE program and Mr. Tony Howell, Director, Educational Opportunity Program at NJIT for the financial support during summer that enabled me to focus on my research. I acknowledge with thanks the input from Ms. Clarisa Gonzalez-Lenahan, Associate Director of Graduate Studies, Mrs. Lillian Quiles, the Administrative Assistant for formatting and improving the presentation of my thesis.

I would like to thank to my seniors: Sarang Muley, Chiranjivi Lamsal and my research group members: Yan Chu, Chang Ge, Nagrajan Chandrasekaran, Aniket Maske and Surmya Sekhri for their support in various aspects during my stay in NJIT.

I am highly indebted to my father, Dr. Vijay S. Nakhate and my mother Vaishali V. Nakhate for being the pillar of my support and blessing throughout my life. I would like to express my gratitude to my siblings, Vikrant Nakhate, Viren Nakhate. I would like to thank the Sinha family who have been my inspiration and helped me since the day I landed in United States of America. I would also like to thank my friends, Venkat Gonguntala and Mrunmayee Phadnis for their endless encouragement and motivation.

TABLE OF CONTENTS

TABLE OF CONTENTS
(Continued)

Chapter

LIST OF FIGURES

LIST OF FIGURES
(Continued)

Figure **Page**

CHAPTER 1

INTRODUCTION

In this thesis, the thermal properties of graphene are investigated. The details of this study are presented in eight chapters.

The second Chapter begins with the basics of graphene. The fundamental properties of graphene and the processing of graphene are explained in this chapter.

The third Chapter of this thesis focuses on the density of states of graphene and the influence of doping on the properties of graphene. This chapter also focuses on the influence of doping on the thermal properties of graphene. A literature survey on the thermal properties is presented in this chapter. Factors that affect the thermal conductivity of graphene are discussed. The basics of heat conduction, phonon dispersion and specific heat of graphene are presented. Specific heat of graphene and graphite is discussed in this chapter.

The fourth Chapter focuses on the thermal transport in graphene. Greeen Kubo method is discussed in this chapter.

The fifth Chapter deals with the computational methods that are utilized to simulate the band structure of materials. Density Functional Theory (DFT) method, Local Density Approximation (LDA) and Pseudopotential (PP) are presented in this chapter.

The sixth Chapter summarizes the software tools and modules that are used for the simulation of the thermal properties. The methods that are used to calculate the phonon modes are highlighted in this chapter.

The seventh Chapter focuses on the results and discussion. The various results, obtained in this study, are discussed and compared with the literature.

The eighth Chapter is the conclusion and recommendations followed by references.

CHAPTER 2

OVERVIEW

Carbon is the base for DNA and all life on earth. It is the most magnificent material in the periodic table. It can exist in many forms and graphite is the most common form. Graphite is made of stacked sheets of carbon.

The two-dimensional (2D) monolayer structure of carbon atoms had been initially considered as unstable. Hence, it was believed that thin 2D films of carbon do not exist. 2D materials have recently been discovered and many researchers have started to investigate them [1]. It has been demonstrated that graphene can be deposited on solid substrates [2]. Graphite is made of many layers of 2D lattices (Figure 2.1). It was believed that single sheet cannot be made from graphite but Russian scientists, Konstantin Novoselov and Andre Geim, discovered graphene which is one atom thick layer of graphite [1]. These scientists received the Nobel Prize in 2010 for their discovery of graphene and its remarkable properties. Graphene samples were initially made by simply etching the substrate off and holding the graphene by its edges [3].

Graphene is a 2D material. Intrinsic graphene is a semimetal with zero band gap. It is an allotrope of carbon and is formed of a lattice of hexagonally arranged carbon atoms. Since 2004, graphene has been studied both experimentally and theoretically. It has excellent properties such as large electrical and thermal conductivity.

Carbon atoms are packed in regular sp^2 bond [4]. Graphene can be rolled into 1D nanotubes, stacked into graphite and wrapped up into zero-dimensional fullerenes (C_{60}). Graphene can be considered as a building block for these carbon allotropes. Figure 2.3

shows the atomic structure of graphene fullerenes and carbon nanotubes. The distance between two carbon atoms is 1.42 Angstrom. Single layer graphene, first demonstrated by Novoselov and Geim, is shown in Figure 2.2. In solid form, graphene has a density of $1g/cm^3$. Stability of graphene is because of its strong covalent planar bonds [5]. Graphene is about 0.34nm thick. It is composed of carbon atoms arranged hexagonally in a honeycomb structure. It has sp^2 bonds which are about 0.14nm long [6]. Carbon has a total of six electrons; two electrons in the inner shell and four electrons in the outer shell. The outer four electrons take part in chemical bonding. In the case of graphene, each carbon atom in planar structure of graphene is bonded to three carbon atoms on the 2D plane. Hence, one electron is free for electronic conduction in 3D. These free electrons are called as pi (π) electrons. These pi electrons are highly mobile. In the case of graphene, these pi orbitals are known to overlap and help in enhancing the carbon-carbon bonds. Graphene with up to ten layers is called Few Layer Graphene [FLG]. More than ten layers of graphene is graphite [7].

The atomic structure of single layered graphene is studied using Transmission Electron Microscopy (TEM). In order to perform TEM on graphene, the layers are generally suspended between two metal grids [8-9].

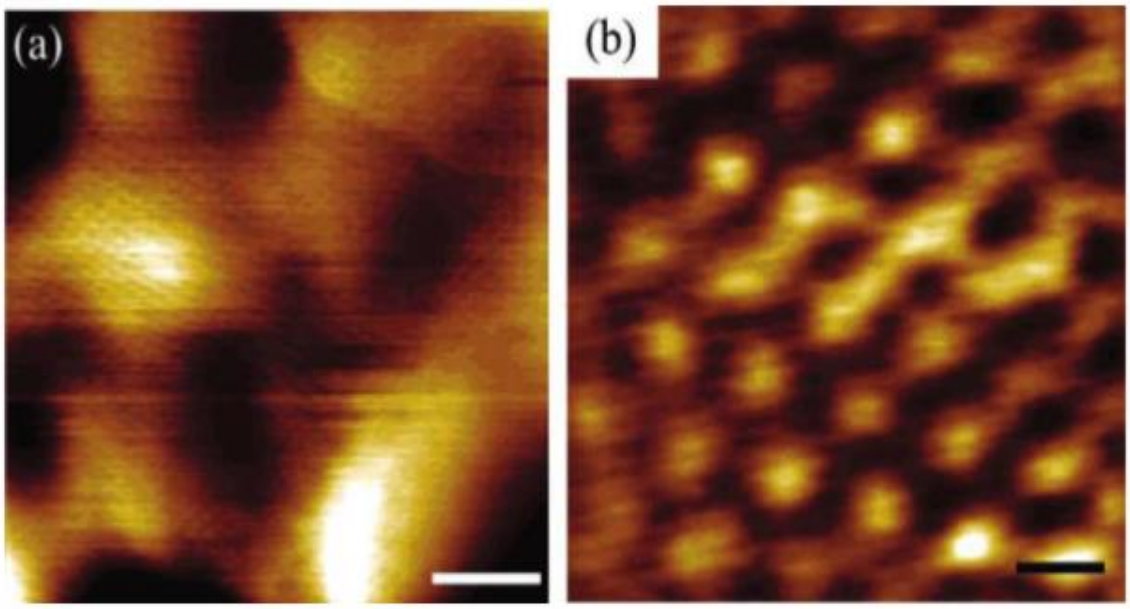

Figure 2.1 (a) STM image of monolayer graphene (b) Atomically resolved image using STM.

Source: M. Ishigami, J. H. Chen, W. G. Cullen, M. S. Fuhrer, and E. D. Williams, *Atomic Structure of Graphene on SiO2*, *Nano. Lett.*, 7 (6) (2007), pp. 1643-1648.

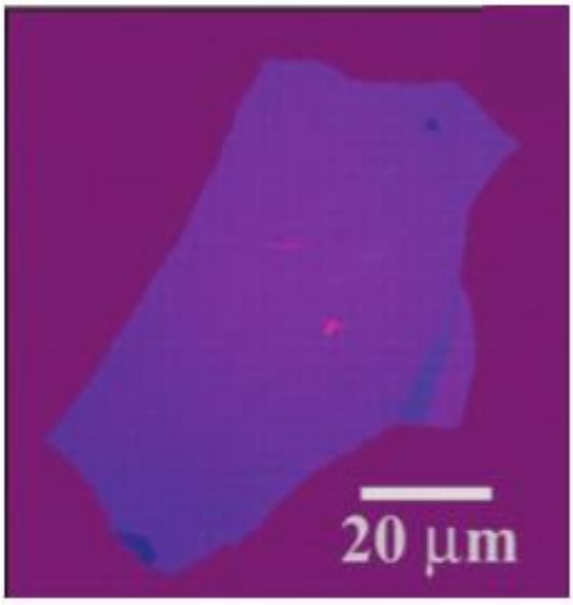

Figure 2.2 Single layer of graphene first demonstrated by the Novoselov and Geim.

Source: K. S. Novoselov, A. K. Geim, S. V. Morozov, D. Jiang, Y. Zhang, S. V. Dubonos, I. V. Grigorieva and A. A. Firsov, *Electric field effect in atomically thin carbon films Sci.*, 306 (5696) (2004) pp. 666-669.

(a) (b) (c)

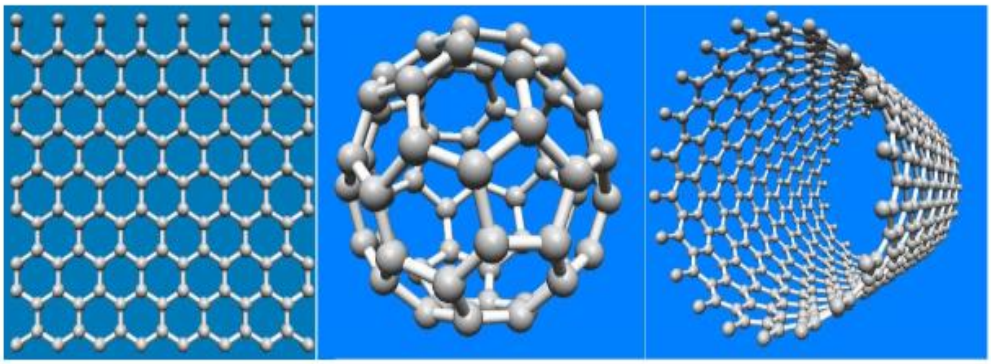

Figure 2.3 (a) Atomic structure of graphene (b) Fullerenes. (c) Carbon nanotubes.

Source: D. Kopeliovich, "*Graphite*" (2013), http://www.substech.com/dokuwiki/doku.php?id=graphite (Accessed 03/26/2015).

Fibrous carbon materials such as carbon composites have been reported to exhibit exceptional mechanical properties such as Young's modulus. They have Young's modulus higher than one TPa in case of carbon nanotubes (CNTs) as well as graphene and fullerene [10-11]. Such unique properties pave way for further research and exploring possibilities for practical applications.

2.1 Graphene Production

It has been suggested that graphene can replace silicon in the very near future due to its large mean free path. However, to produce graphene commercially has been a major obstacle. The main challenge is to be able to synthesize and process graphene in bulk quantities. Graphene is known to form irreversible agglomerates to form graphite through Vander Waals interaction unless the layers are well separated from each other.

Various top down approaches have been utilized to make single layer graphene. Bottom up approaches such as epitaxial growth of graphene on SiC substrate, Chemical Vapor Deposition (CVD) etc. have also been implemented.

2.1.1 Mechanical Exfoliation

Graphene was first obtained in 2004 through mechanical exfoliation method. Novoselov and Geim prepared graphene by peeling off thinner graphite flakes from bulk graphite. The graphene flakes were deposited on Si-SiO_2 substrates at sizes of approximately $10\mu m^2$[12]. They used a scotch tape for the same. These scientists repeated the process until they got one-dimensional (1D) graphene. Graphite is many layers of graphene stacked together. The sp^2 bonding between carbon atoms in graphene is very strong. The bonding between two graphene layers is due to Vander Waals force. This force is very weak and can be easily broken by external forces. This process of obtaining graphene is called mechanical exfoliation [13]. However, this process is time consuming and requires lot of man power. Graphene flakes of around 100 micrometer can be obtained by this process. Graphene prepared by this method is still widely used. The thickness of graphene obtained by this method cannot be controlled and uniform graphene cannot be obtained from this method. Hence, graphene prepared by this method has limited use.

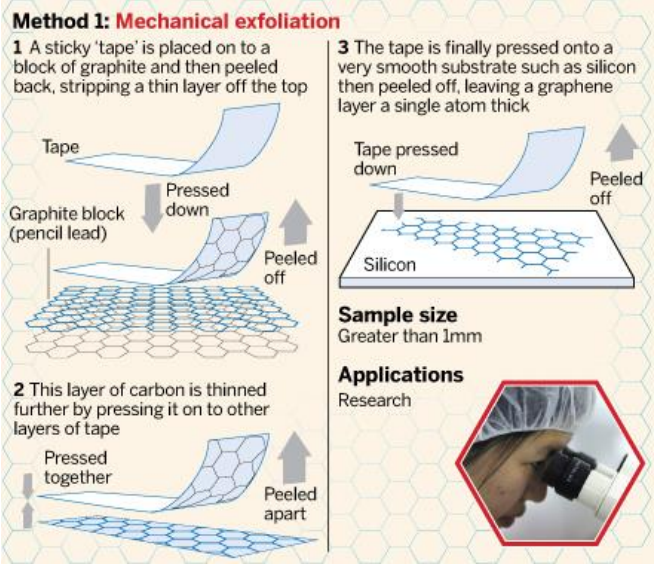

Figure 2.4 Mechanical exfoliation of graphene.

Source: *"Graphene: Faster, Stronger, Bendier"* (2013), http://www.ft.com/cms/s/0/6f4717b6-66f9-11e2-a83f-00144feab49a.html (Accessed 03/24/2015).

2.1.2 Chemical Vapor Deposition

Layers of graphene have been synthesized by this method on metal substrates and then successfully transferred to various substrates. CVD is a process in which an epitaxial layer can be formed. Graphene, grown by this method, has numerous potential applications in the semiconductor industry. The graphene obtained by this method is highly pure. In this method, a carbon source is used in the reaction chamber where it reacts with the metal substrate and a material film is obtained on the substrate. The temperature of the substrate, the reactants, the chemical reaction, the gaseous products, the reaction products play important role and define the type of reaction that will occur. During the CVD process, the toxic by-products are removed from the reaction chamber. The epitaxial method produces graphene by removing silicon atoms from silicon carbide wafers. Using metals as the catalyst, graphene is also produced on nickel sheets. Figure 2.5 shows that high quality graphene films can be produced on nickel substrates under

ambient pressure. The produced film is transferred onto arbitrary substrates through etching of metal layers [14-15]. Methane is used as a source for carbon. After etching the metal, a substrate is brought in contact with the graphene film and it is pulled from the solution. In another method, graphene is coated with polydimethylsiloxane (PDMS) or poly-methyl methacrylate (PMMA). After this step, the metal is dissolved and graphene is lifted from the solution [16-17-18].

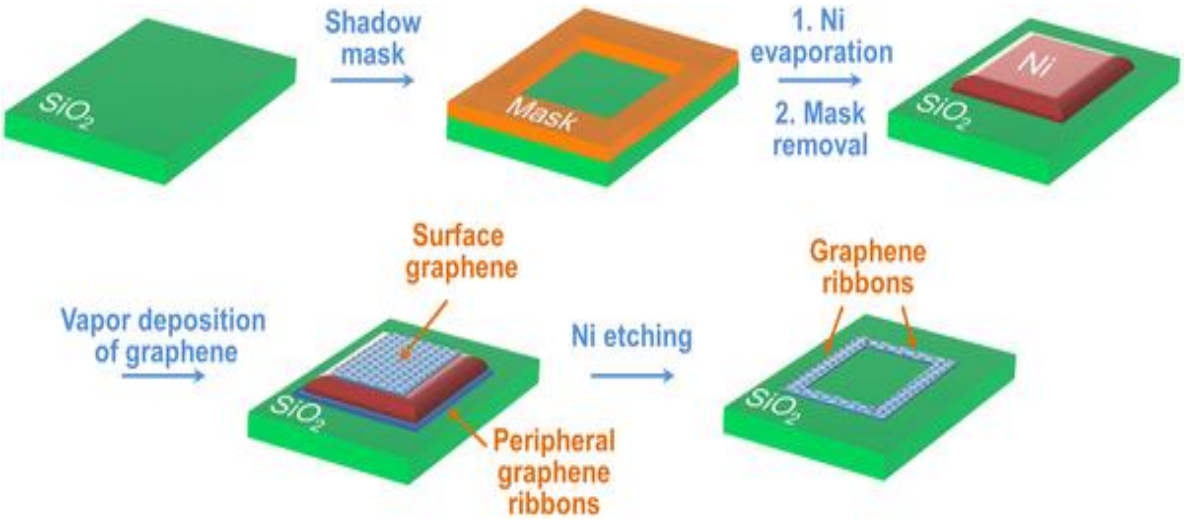

Figure 2.5 Graphene obtained by CVD on SiO_2 substrate.

Source: D. Wang, Y. Yang, D. Xie, T. Ren and Y. Zhang, *Scalable and Direct Growth of Graphene Micro Ribbons on Dielectric Substrates, Sci. Reports*, (2013), pp. 1348.

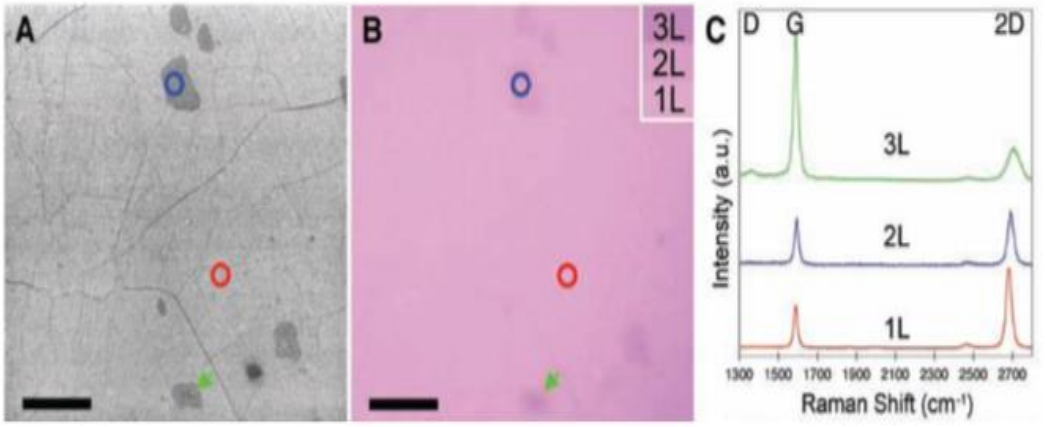

Figure 2.6 (a, b) Graphene grown by chemical vapor deposition (c) Raman spectra of graphene.

Source: X. Li, W. Cai, J. An, S. Kim, J. Nah, D. Yang, R. Piner, A. Velamakanni, I. Jung, E. Tutuc, S. K. Banerjee, L. Colombo and R. Ruoff, *Large-area Synthesis of High-Quality and Uniform Graphene Films on Copper Foil*, *Sci*., 324 (2009), pp.1312-1314.

In the case of graphene, two peaks are created due to the Stokes phonon energy shift by laser excitation. A primary in-plane vibrational mode ($1580cm^{-1}$) and a second-order overtone of a different in-plane vibration peaks are created. D and 2D peaks are dependent on the laser excitation energy [19-20]. As the number of layers increases, the splitting of 2D peaks occurs. The 2D peak is split into number of modes; as a result, we can get a number of wider, shorter, higher frequency peaks. The increasing number of layers can also cause a smaller red shift of the G peak. Figure 2.6 (c) shows the Raman spectra from various spots of a CVD graphene film grown on Nickel [21].

CHAPTER 3

THERMAL PROPERTIES OF GRAPHENE

3.1 Density of States

The density of states represents the number of energy states in a solid. One-dimensional density of states of electrons represents the number of electron states per unit length per $\boldsymbol{dk}$ in the Brillouin zone ($\boldsymbol{k}$ is the wave vector). In case of three dimensional structures, the density of states of phonons represents the number of phonon states per unit volume $\boldsymbol{d\omega}$. The distance between two Brillouin edges is $\frac{\boldsymbol{2\pi}}{\boldsymbol{a}}$. The density of states of the solid, with $\boldsymbol{n}$ dimensions, D_{nD} is given as [22]:

$$D_{nD} = \frac{(n-1\ surface\ of\ n-dimensional\ space)dk}{(\frac{2\pi^n}{a})L^n dk} \tag{3.1}$$

where, L^n is the volume of unit space n. Density of states per energy interval is as follows:

$$D_{nD} = \frac{(n-1\ surface\ of\ n-dimensional\ space)dk}{(\frac{2\pi^n}{a^n})L^n d\epsilon} \tag{3.2}$$

The equation 3.2 is used for calculating the thermal properties. It can be used in phonon dispersion relations and it is done by solving the dispersion relation for k.

The electron dispersion relation can be written as follows:

$$k = \sqrt{\frac{2m\epsilon}{h^2}} \tag{3.3}$$

The equation 3.3 leads us to the following:

$$\partial k = \frac{1}{2}\sqrt{\frac{2m\epsilon}{h^2\epsilon}}\partial\epsilon \tag{3.4}$$

From the phonon dispersion relation, we get:

$$k = \frac{\omega}{v_g} \tag{3.5}$$

Therefore,

$$\partial k = \frac{\partial\omega}{v_g} \tag{3.6}$$

In case of 1D solids, the density of states is given as follows:

$$D = \frac{dk}{\left(\frac{2\pi}{a}\right)Ld\epsilon} \tag{3.7}$$

Therefore, the 1D electron density is as follows:

$$D_e = \frac{1}{2\pi}\sqrt{\frac{2m}{h^2\epsilon}} \tag{3.8}$$

As a result, the 1D phonon density of states is given by:

$$D_p = \frac{1}{2\pi v_g} \tag{3.9}$$

The 2D density of states is given by:

$$D_{2D} = \frac{2\pi k dk}{(\frac{2\pi}{a})^2 L^2 d\epsilon} \tag{3.10}$$

The electron density of states for two dimensions is given by:

$$D_{e,2D} = \frac{1}{\pi}\frac{m}{h^2} \tag{3.11}$$

The 2D phonon density of states is given by:

$$D_{p,2D} = \frac{\omega}{\pi {v_g}^2} \tag{3.12}$$

The three-dimensional (3D) density of states is given by:

$$D_{3D} = \frac{4\pi k^2 dk}{(\frac{2\pi}{a})^3 L^3 d\epsilon} \tag{3.13}$$

The electron density of states is given as follows:

$$D_{e,3D} = \frac{1}{2\pi}(\frac{2m}{h^2})^{\frac{3}{2}}\epsilon^{\frac{3}{2}} \tag{3.14}$$

The 3D phonon density of states is given as follows:

$$D_{p,3D} = \frac{3\omega^2}{2\pi^2 v_g^3} \tag{3.15}$$

3.2 Doping of Graphene

Graphene is a zero band gap semiconductor. The carrier concentration of the carbon layer must be adjusted to facilitate the transport in graphene based devices. This can be done by adjusting the Fermi level away from the Dirac point where the density of states is zero [23]. It can be done by chemical doping or electrostatic gating. It is shown in Figure 3.1. It can be done by chemical doping or electrostatic gating [24]. In conventional semiconductors, doping is achieved by substitution of charge donating species. The binding energy of the dopant Rydberg states is reduced by the square of the dielectric constant. Hence, dopant ionization takes place at room temperature. In case of graphene, which is a 2D structure, the doping precludes this bulk mechanism. The doping of graphene can be done by a variety of chemical means. Hole (p) or electron (n) doping can be achieved by contacting the carbon layer with different metals. Boron or nitrogen can be directly substituted into the carbon lattice by removing or donating electrons [25-26]. Graphene can also be doped by adsorption of chemical species on its surface. This process helps in enhancing the electrical properties of carbon based electronics [27-28].

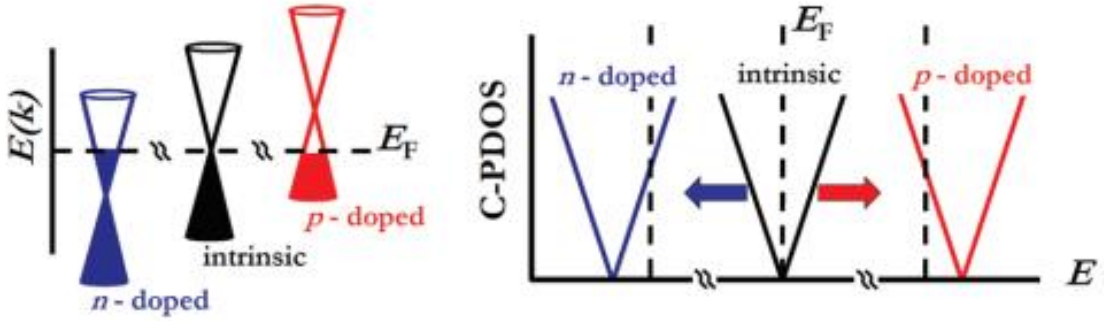

Figure 3.1 The doping mechanism in graphene.

Source: G. Jo, M. Choe, S. Lee, W. Park, H. Y. Kahng and T. Lee, *The application of graphene as electrodes in electrical and optical devices, IOP Sci., Nanotech.,* 23 (11) (2012).

3.3 Significance of Thermal Properties of Graphene

In this section, the phonon transport in graphene is discussed. The two-dimensional phonon transport and its relation to heat conduction is described.

In the literature, the study of thermal properties of materials has seen rapid growth in recent years. Self-heating is a crucial issue. Hence, heat removal is of significant importance in the electronics industry. The quanta of lattice vibrations, that is phonons, are the main reason for heat conduction in materials. Carbon and its allotropes have unique ability to conduct heat. Bulk structures show different thermal properties as compared to nanostructures. In semiconductor nanowires, as well as in thin films, there is phonon boundary scattering [29]. In most of the solids, heat which is carried by phonons is also scattered by impurities, other phonons, lattice defects and interfaces. Theoretical studies of heat conduction reveal that phonon transport in 2D or 1D have exotic behavior and hence results in high thermal conductivity [30].

The thermal properties of graphene are derived from those of graphite and bear the imprint of the highly anisotropic nature of the crystal [31]. Atomic structure plays an important role in materials ability to conduct heat. Material of a nanometer scale shows different thermal properties. Validity of Fourier law is very important in low-dimensional systems. Carbon and its wide range of allotropes have unique thermal properties. Thermal conductivity of different allotropes are 0.01 WmK^{-1} for amorphous carbon and more than 2000 WmK^{-1} at room temperature for graphene [32].

The measurements of thermal properties of graphene has led to more interest in this material and eventually heat conduction in lower dimensionality crystals. In Figure 3.2, the thermal conductivity (K) values for sp^2 bonding, sp^3 bonding and disordered mixture of sp^2 and sp^3 is shown [33].

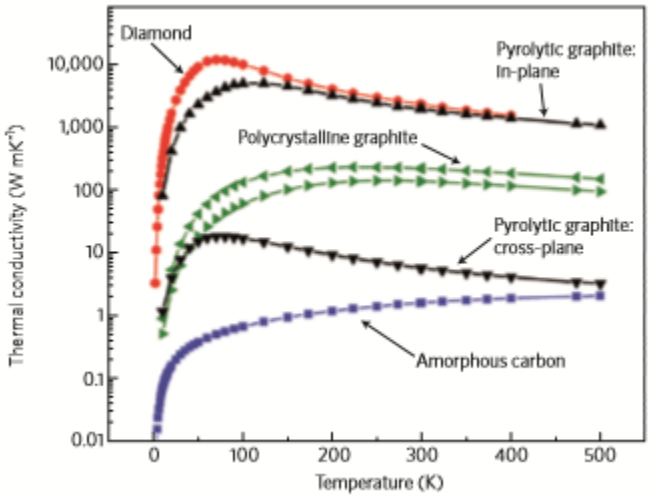

Figure 3.2 Thermal conductivity of bulk carbon allotropes as a function of temperature.

Source: C. Y. Ho, R. W. Powell and P. E. Liley, *Thermal conductivity of the elements: a comprehensive review*, *J. Phys. Chem. Ref. Data*, 1 (2) (1972).

The Vander Waals interactions limit the heat flow in the cross-plane direction of graphene and graphite. In Figure 3.2, the thermal conductivity curve for diamond is for electrically insulating type-II diamond. Very high purity pitch-bonded graphite is called as polycrystalline graphite. There is significant difference in thermal conducitivity between pyrolytic graphite and polycrystalline graphite because of disoriented grains. At low T, K is proportional to Tγ, where γ varies over a wide range depending on graphite's quality and crystallite size [33].

3.4 Basics of Heat Conduction

It is important to discuss the nanoscale size effects on heat conduction. The thermal conductivity is defined by Fourier's Law:

$$q = -K\nabla \mathrm{T} \tag{3.16}$$

where, q is the heat flux, K is the thermal conductivity, ∇T = temperature gradient. K is constant for small temperature variations. K is a function of T in the wide temperature range. Acoustic phonons play a major role to carry heat in solid materials, which are ion-core vibrations in a crystal lattice and electrons. Therefore,

$$K = Kp + Ke \tag{3.17}$$

where, Kp is the phonon contribution to thermal conductivity, Ke is the electron contribution to thermal conductivity; Ke is dominant in metals since metals have larger

concentration of free carriers. The electrical conductivity is defined by Wiedeman - Frenz law as follows:

$$\frac{K_c}{\sigma T} = \frac{\pi^2 k_b 2}{3e^2} \tag{3.18}$$

where, Kb is the Boltzmann Constant, e is the charge of an electron. Phonons dominate heat conduction in graphite which also has metal like properties [34]. It is due to the strong covalent sp^2 bonding resulting in efficient heat transfer by lattice vibrations. To distinguish between diffusive and ballistic phonon transport is important. In the case of diffusive transport, the size of the sample, L, is much larger than phonon mean free path. When phonon mean free path is larger than L, the thermal transport is termed as ballistic. Fourier's law assumes diffusive transport. Due to the crystal lattice anharmonicity, the thermal conductivity is called intrinsic. When the crystal is defect free, i.e., without defects and impurities, phonons cannot be scattered by other phonons and the intrinsic thermal conductivity reaches its limit [35, 36]. The thermal conductivity is limited by extrinsic factors such as phonon-rough-boundary or phonon defect scattering. The equation for phonon thermal conductivity is as follows:

$$K_p = \sum C_j \int C_j(\omega) v_j 2(\omega) \tau_j(\omega) d\omega \tag{3.19}$$

where, $v_j = \frac{d\omega_j}{dq}$ is the velocity of the j^{th} branch, τ_j is the phonon relaxation time, C_j is the heat capacity of the j^{th} branch.

In pure crystals, phonon mean free path is limited by the phonon scattering which is due to crystal anharmonicity. This is called the Umklapp scattering where thermal conductivity is limited [37]. The thermal conductivity in such cases is called as intrinsic. In case of extrinsic thermal conductivity, the phonon scattering is due to extrinsic effects such as phonon-rough boundary or defect scattering.

In nanostructures, the phonon group velocity decreases due to the quantization of phonon energy spectra. There is a decrease in thermal conductivity due to the change in phonon energies, density of states and change in group velocity. In case of nanostructures, the thermal conductivity can be increased by spatial confinement of acoustic phonons [38, 39]. We can evaluate the phonon boundary scattering and it is given by the following equation [40]:

$$\frac{1}{\tau_{Bj}} = \frac{v_j}{D}\frac{1-p}{1+p} \tag{3.20}$$

where, D is the grain size, p is the probability of scattering and is given by:

$$p(\lambda) = \exp(-\frac{16\pi^2\eta^2}{\lambda^2}) \tag{3.21}$$

where, η is the root mean square deviation of the height of the surface from the reference plane, λ is the length of the incident phonon wave.

In case of nanostructures, the mean free path of phonons is very high. In such cases, there is quantization of phonon spectra; hence, the thermal conductivity dependence on the physical structure becomes complicated [40].

The specific heat depends on the density of states. Hence, specific heat depends on the dimensionality – i.e., 1D, 2D, or 3D structures which are also reflected in the thermal conductivity at low temperature. [40, 41]. In the case of 2D materials, the thermal conductivity is directly proportional to square of temperature.

The thermal diffusivity also plays an important role which determines how quickly the material will get heated. It is given by the following equation:

$$\alpha = \frac{K}{C_p \rho_m} \tag{3.22}$$

where, ρ_m is the density of the material. The thermal conductivity which depends on phonons is also affected when the structure is three dimensional (3D).

3.5 Phonon Dispersion in Graphene

The unit cell of graphene is shown in Figure 3.3. It is shown by dashed lines and it contains N=2 carbon atoms which leads to formation of three acoustic (A) and three optical (O) phonon modes. The phonon dispersion spectra is shown in Figure 3.4. It is based on the relation $E = \hbar\omega$ where $\hbar$= Planck's constant, E =Phonon energy and ω is the frequency. In case of graphene, which is 2D in nature, out of plane atomic displacement takes place. It is called as flexural (Z) phonons. The flexural out of plane acoustic (ZA) modes are responsible for the unusual thermal properties of graphene. The areal density of carbon atoms in graphene atoms is $3.82*10^{15}$ cm^{-2} [42].

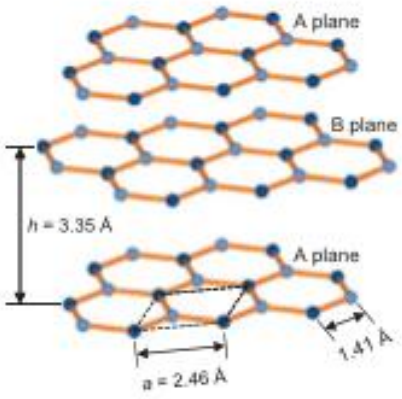

Figure 3.3 Atomic arrangement of graphene sheets. The outline of unit cell is represented by dashed lines.

Source: E. Pop, V. Vashney and A. K. Roy, *Thermal Properties of graphene: Fundamentals and applications*, 37 (2012), pp. 1273-1281.

The flexural out of plane acoustic (ZA) modes are responsible for the unusual thermal properties of graphene.

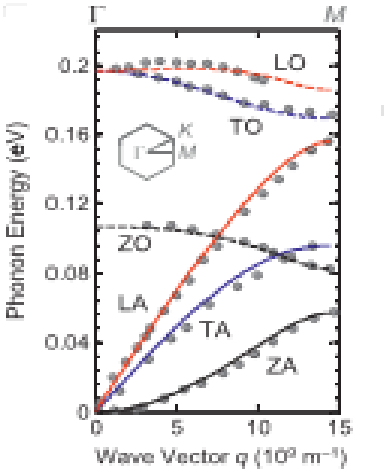

Figure 3.4 Phonon dispersion of graphene.

Source: E. Pop, V. Vashney and A. K. Roy, *Thermal Properties of graphene: Fundamentals and applications*, 37 (2012), pp. 1273-1281.

3.6 Specific Heat of Graphene

The change in energy density U, when the temperature changes by 1K, is called specific heat, C, of a material. It is represented by [42]:

$$C = \frac{du}{dT} \tag{3.23}$$

where, T is the absolute temperature. The specific heat also represents how quickly a body cools or heats. The specific heat is given by $C = Ce + Cp$ where the specific heat is stored by the lattice vibrations and free conduction electrons of a material. The phonon specific heat increases as the temperature of the material increases [43, 44]. At very high temperatures, the specific heat becomes constant and this is also called as Dulong-Petit limit which is shown in Figure 3.4. In case of graphite, the specific heat is around 30% higher than that of diamond because of the weak coupling between the graphite layers [45]. In case of graphene, when its flexural mode is thermally excited, it shows similar behavior. The phonon contribution is obtained by integrating over the phonon density of states with a convolution factor. The convolution factor reflects the energy and occupation of each state. It is shown in the equation 3.24 [46]:

$$C_{ph} = \int_0^{\omega_{max}} k_B \left(\frac{\hbar\omega}{K_B T}\right)^2 \frac{e^{\frac{\hbar\omega}{K_B T}}}{\left(e^{\frac{\hbar\omega}{K_B T}} - 1\right)^2} \rho(\omega) d\omega \tag{3.24}$$

The above relation reflects the occupation and energy of each phonon state where $\rho(\omega) =$ phonon density of states, $\omega_{max} =$ highest phonon energy of the material. When

ω =0, the convolution factor is 1 and decreases to a value of ~0.1 at $h\omega = \frac{K_B T}{6}$. As the temperature is increased, the phonon specific heat increases. At moderate temperatures, the specific heat cannot be calculated analytically. At low temperatures, $\rho(w)$ is dominated by acoustic phonons. Thus, we get the information of phonon dispersion and dimensionality of the system from the specific heat at low temperatures [46].

The specific heat of a material is dependent on temperature. At low temperatures, the specific heat C_p is directly proportional to $T^{\frac{d}{n}}$ for phonon dispersion in the d dimensions [47, 48]. It yields information on the dimensionality and phonon dispersion. The phonon ZA modes dominate at low temperatures; then the specific heat is proportional to T^2. The LA and TA phonons dominate at high temperature. Debye temperature is obtained when there is flattening of the phonon spectra [42]. This corresponds to high temperatures. It is shown in Figure 3.5; for temperatures below 50K, the specific heat for graphene is linear with temperature T. But, for graphite, below 10K, the specific heat is proportional to the cube of temperature. This is due to the weak interlayer coupling. Once the soft c-axis modes are filled up, the specific heat is proportional to the square of temperature.

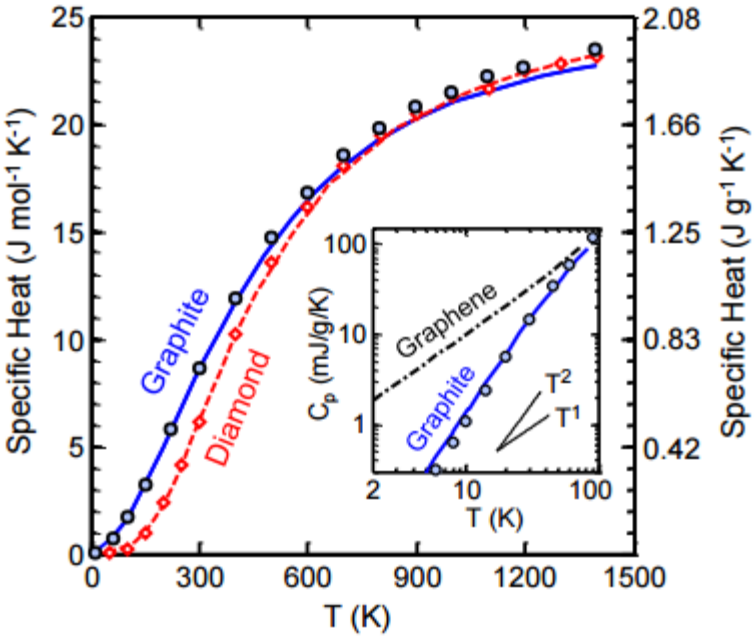

Figure 3.5 Specific heat of graphite, diamond, graphene versus temperature.

Source: E. Pop, V. Vashney and A. K. Roy, *Thermal Properties of graphene: Fundamentals and applications*, 37 (2012), pp. 1273-1281.

3.7 Thermal Conductivity of Graphene

Figure 3.6 shows that the thermal conductivity of graphene is around 2000-4000 $Wm^{-1}K^{-1}$ for free-standing samples (not attached to substrate) [49]. The thermal conductivity of graphene is compared to the thermal conductivity of diamond. The thermal conductivity of diamond is around 2200 $W^{-1}K^{-1}$. The thermal conductivity of other materials at room temperature is shown in Figure 3.7. Weak Vander Waals interactions are present for the heat flow in the cross-plane direction which results in limited heat flow. As shown in Figure 3.7, the specific heat of graphite at room temperature is around 6 $Wm^{-1}K^{-1}$. In case of graphene, the heat flow perpendicular to the graphene sheet is limited by weak Vander Waals force interactions with adjacent substrates.

The ballistic thermal conductance of graphene can be numerically calculated from phonon dispersion and is shown in Figure 3.6. At low modes, the flexural ZA modes dominate at low temperatures and the specific heat is directly proportional to $T^{1.5}$ and the phonon dispersion with $\omega = q^2$. The thermal conductivity of graphene is ballistic when the phonon mean free path is more than the length of graphene. The phonon mean free path is around 600nm [42]. The thermal conductivity is diffusive when the phonon mean free path is less than the length of graphene.

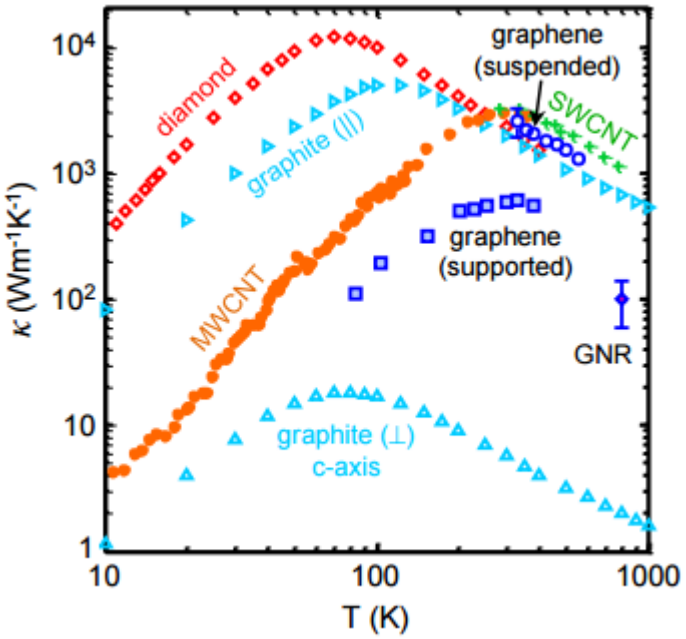

Figure 3.6 Thermal conductivity of graphene and other carbon materials versus temperature.

Source: E. Pop, V. Vashney and A. K. Roy, *Thermal Properties of graphene: Fundamentals and applications*, 37 (2012), pp. 1273-1281.

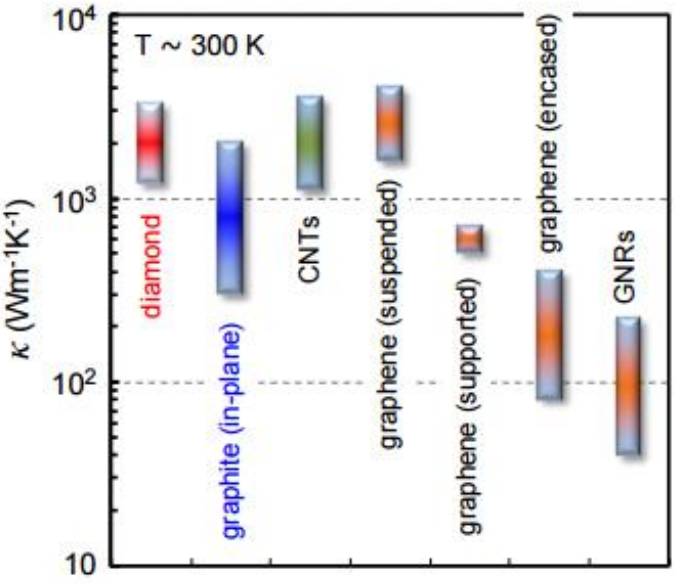

Figure 3.7 Room temperature ranges of thermal conductivity data *K* for various carbon structures.

Source: E. Pop, V. Vashney and A. K. Roy, *Thermal Properties of graphene: Fundamentals and applications*, 37 (2012), pp. 1273-1281.

CHAPTER 4

THERMAL TRANSPORT IN GRAPHENE

Electronic devices are shrinking day by day and, with their shrinking size, the materials to materials interface become extremely important. The thermal properties depend on the interface between materials. In the case of materials at the nanoscale, the interface thermal resistance affects the thermal conductivity of the material. As heat dissipation is a major concern in nanoscale devices, the materials (and its choice) also play an important part in device applications.

The thermal conductivity of graphene is difficult to be determined experimentally; hence the thermal conductivity is mostly predicted from theoretical methods. Non-equilibrium dynamics is the most intuitive theoretical method for determining the lattice thermal conductivity. In this method, the thermal conductivity is calculated from the ratio of the heat flux to a temperature gradient. In the simulation method, a heat flux is imposed and the resulting temperature gradient is calculated or heat flux required to maintain it is calculated when the fixed temperature gradient is imposed [50].

Molecular Dynamics (MD) simulations are performed in conjunction with a periodic simulation cell. In this method, the simulation cell is divided into an even number of equal sections - one as the hot section and another as the cold section. The heat is transferred from the cold section to the hot section and at regular intervals of time. Since the simulation cell is periodic, heat leaves the side of the hot section and enters the side of the cold section leading to two heat fluxes in opposing directions and corresponding temperature gradients. Several models have been tested to investigate the

thermal conductivity of graphene. The thermal conductivity is determined through phonon dispersion and has values in the range of 2000 W/mK to 5000W/mK.

There are number of methods for calculating the thermal conductivity. One of the most popular methods is to transfer the heat from the hottest atom in the cold section to coldest atom in the hottest section. This method is called as Muller-Plahte method [50]. It is also called as reverse non-equilibrium molecular dynamics (R-NEMD).

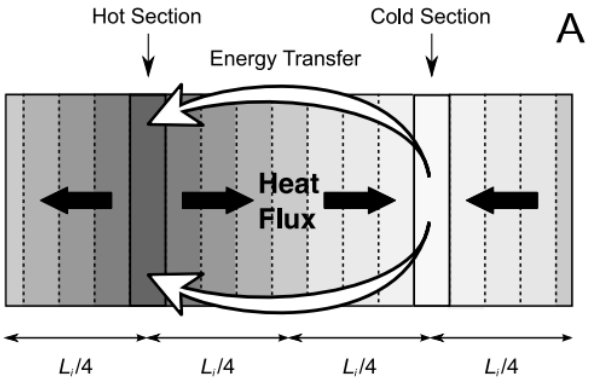

Figure 4.1 Typical set up in a non-equilibrium molecular dynamic simulation.

Source: S. Stackhouse, *Theoretical Methods for Calculating the Lattice Thermal Conductivity of Minerals*, 71 (2010), pp. 253-269.

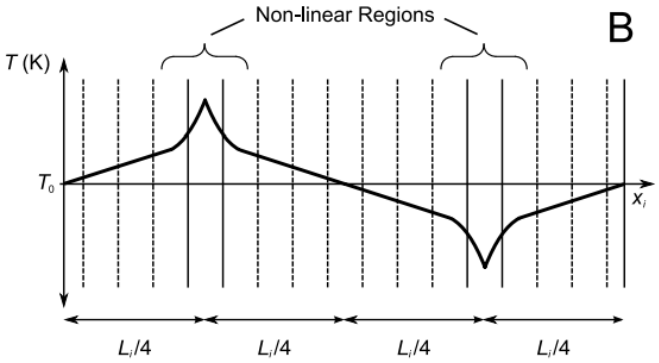

Figure 4.2 Temperature profile.

Source: S. Stackhouse, *Theoretical Methods for Calculating the Lattice Thermal Conductivity of Minerals*, 71 (2010), pp. 253-269.

The hottest atom in the cold section is assumed to undergo an elastic collision with the coldest atom in the hot section at regular intervals. The velocities assigned to the atoms, before collision and post-collision, are determined in the simulation. The post collision velocity of the atom in the cold section is calculated as [50]:

$$v_c' = -v_c + 2 * \frac{m_c v_c + m_h v_h}{m_c + m_h} \tag{4.1}$$

The velocity of the atom in the hot section is calculated as:

$$v_h' = -v_h + 2 * \frac{m_c v_c + m_h v_h}{m_c + m_h} \tag{4.2}$$

where, m_c is the mass of the atom in cold section, m_h is the mass of the atom in the hot section and v_c, v_h is the velocities of the atoms in the hot section and cold section before collision and v_c', $v_h'$is the velocity of the atom after collisions. The average heat flux is determined from [50]:

$$q_i = \frac{1}{2AN\Delta t} \sum_{n=1}^{\frac{N}{v_t}} \frac{1}{2} m_h (v_h'(n{v_t}^2 - v_h(n{v_t}^2)) \tag{4.3}$$

where, q_i is the average heat flux flowing in the i direction, A is the cross sectional area which is perpendicular to i, N is the total number of time steps, v_t is the frequency of transfers in time steps. In the above equation, heat flows from both sides of the hot section to both sides of the cold section and the average of half of the exchanged

heat flowing in each of the two directions is considered. The magnitude of heat flux and the corresponding temperature gradient can be controlled by varying the frequency of heat transfers.

In another approach, the whole system is divided into slabs along the axial direction, and the temperature of each slab is calculated [50].

$$T_s = \frac{1}{3k_bN}\sum_{i=1}^{N} m_i \, {v_i}^2 \tag{4.4}$$

In this technique, the first layer is considered as hot layer and the middle layer is considered as cold layer. The hottest atom with the highest kinetic energy exchanges its energy with the adjacent atoms till the heat energy reaches the atom with minimum kinetic energy. The temperature gradient is very broad. Hence, the hottest atom at the cold section has the highest kinetic energy. The linear momentum and the energy of the system is conserved and the angular momentum is not conserved. However, the angular momentum can be neglected since the introduction of periodic boundary.

4.1 The Green-Kubo Method

In this method, the entire lattice thermal conductivity can be calculated from one simulation. This is exactly opposite to non-equilibrium molecular dynamics method in which several simulations needs to be considered in various directions. In this method, there is less experimental work because the effect of section size or heat flux is not considered in the results. This method is for the most part limited to the study of those phases which are well described by a set of empirical pair potentials.

In equilibrium molecular dynamics, the system which is under investigation has constant average temperature and the average heat flux is zero. Due to fluctuations of temperature, a finite heat flux exists. In this method, there is a relation between lattice thermal conductivity of the system to time required for such fluctuations to dissipate.

$$k_{ij} = \frac{V}{k_b T^2} \int_0^\infty < q_i(0) q_j(t) > dt \tag{4.5}$$

where, T is the temperature of the system, $q_i(0)$ the instant heat flux in the $j$direction at time zero and $q_j(t)$ the instantaneous heat flux in the i direction at time t. In a molecular dynamics study, we consider time steps and thus, we consider the following equation

$$k_{ij} = \frac{V\Delta t}{k_b T^2} \sum_{m=1}^{M} (N-m) \sum_{n=1}^{N-m} q_i\,(m+n) q_j(n) \tag{4.6}$$

where, N is the total number of time steps, $q_j(n)$ the instantaneous heat flux in the $j$direction at time-step n, $q_i(m+n)$ the instantaneous heat flux in the i direction at time step $(m+n)$.

The energy is the total of kinetic and potential energy of each atom.

$$\varepsilon_i = \frac{1}{2} m_i {v_i}^2 + \frac{1}{2} \sum_j^N u_{ij}\,(r_{ij}) \tag{4.7}$$

where, m_i is the mass of atom i, v_i the velocity vector of atom i.

CHAPTER 5

COMPUTATIONAL METHODS

5.1 Density Functional Theory

The density functional theory is used to calculate the electronic structure of matter. It is used in many fields to calculate the ground state of many body systems and electron density plays an important role. Its application ranges from molecules, atoms, solids, quantum and classical fields.

Solving Schrodinger's equation gives solutions to many ab-initio techniques. In order to describe arbitrary systems accurately, it is very important to solve this equation but we need to consider approximations. In the time-independent, non-relativistic Schrodinger equation, a Hamiltonian is used to describe a system containing nuclei and electrons. In this method, the system is considered as a homogenous electron gas and Fermi-Dirac statistics are applied. The model considers the electrostatic interaction between the nuclei and the electrons. The equation provides a relation between the potential and electronic density. We cannot predict chemical bonding of atoms by using the Schrodinger equation.

Another approach is by the Hartree-Fock method which was developed to solve the time independent Schrodinger equation. It is the basis of molecular orbital theory [51]. It is assumed that electron motion can be considered as single particle function. The accuracy is not much in this method. This method is used in case of periodic systems.

The equation can be written as follows:

$$V_{HF}(x_1) = \sum_j^N (J_j(x_1) - K_j(x_1)) \tag{5.1}$$

where, V_{HF} is the Hartree-Frock potential which is dependent on the spin orbitals. DFT is the widely used method. In this method, the system is described by its particle density. Wave function is not considered. Hence, the system is reduced to fewer coordinates via its particle density. DFT is dependent on Hohenberg-Kohn theorems [52]. The density of states plays an important role in determining the ground state of many systems and the second theorem states that the variation principle can be used to calculate this quantity. The ground state is a function of density. Physical properties and energy are function of density.

Density functional theory depends on two mathematical theorems proposed by Kohn and Hohenberg. The first theorem states that "*The ground state energy from Schrodinger's equation is a unique functional of the electron density"* [52]. It is used to calculate the Hamiltonian operator. There is mapping between electron density and wave function. In a way, ground state energy can be expressed as:

$$E[n(r)] \tag{5.2}$$

where, $n(r)$ is the electron density. The ground state electron density determines energy and wave function of the ground state.

However, the first theorem proposes that the electron density can be considered to solve the Schrodinger equation; it does not say anything about the functional. In the second theorem of Hohenberg-Kohn, it states that "*The electron density that minimizes the energy of the overall functional is the true electron density corresponding to the full solution of the Schrodinger equation"* [52].

The functional can be written in terms of single electron wave functions. The energy functional is, therefore, as follows:

$$E[\{\psi_i\}] = E_{known}[\{\psi_i\}] + E_{XC}[\{\psi_i\}] \tag{5.3}$$

In the above equation, we have split the functional in a simple form where we can further write the above equation as follows [53]:

$$E_{known}[\{\psi_i\}] = \frac{h^2}{m}\sum_i \int \psi_i \nabla^2 \psi_i d^3r + \int V(r)n(r)d^3r + \frac{e^2}{2}\int\int \frac{n(r)n(r')}{r\ r'}\ d^3r\ d^3r' + E_{ion} \tag{5.4}$$

where, the equation on the right hand side shows the electron kinetic energies, the Coulomb interactions between the electrons and the nuclei, between the pairs of electrons and the interactions between the pairs of nuclei.

E_{XC} is the exchange correlation functional. It describes the quantum mechanical effects. To calculate the electronic properties, Hohenberg-Kohn theorem provides basis of the ground state density of the system. However, it is not possible to calculate the ground state energy. Hence, we have to consider Kohn-Sham equations from which the

ground state energy can be calculated. In order to do so, it should be assumed as a functional of charge density. The Kohn-Sham equation is given as [54]:

$$\left[\frac{-\hbar^2}{2m}\nabla^2 + v_{eff}(r)\right]\Psi_i(r) = \in_i \Psi_i(r) \tag{5.5}$$

where, $\in_i$ is the energy of the orbit [55].

$$v_{eff}(r) = V(r) + V_H(r) + V_{XC}(r) \tag{5.6}$$

where, (r) is the potential that defines the interaction between an electron and atomic nuclei; $V_H(r)$ is the Hartree potential and is written as:

$$V_H(r) = e^2 \int \frac{n(r\prime)}{r\ r'} d^3r' \tag{5.7}$$

The Hartree potential describes the electron density of all the electrons:

$$V_{XC}(r) = \frac{\delta E_{XC}(r)}{\delta n(r)} \tag{5.8}$$

where, V_{XC} is the functional derivative of the exchange correlation energy.

5.2 Basis Set

A basis is used to build molecular orbitals which are created by combining linear functions.

5.2.1 Slater Type Orbitals

Slater type orbitals are named after the physicist John Slater. It is used to calculate basis functions. It gives the Eigen functions of the hydrogen atom. It is given by:

$$\emptyset_{abc}^{STO}(x,y,z) = Nx^a y^b z^c e^{-\zeta\Upsilon} \tag{5.9}$$

where, N is the normalization constant, ζ is the width of the orbital. In equation 5.9, the angular momentum is controlled by a,b,c.

However, in computational methods, STO is not used that much because the integrals are difficult to compute.

5.3 Local density Approximation

Local density approximation is highly used in DFT to determine the exchange-correlation energy functional. LDA is given by [53]:

$$E_{xc} = \int dr\rho(r)\epsilon_{xc}\big(\rho(r)\big) \tag{5.4}$$

where, E_{xc} is the exchange correlation energy per electron in a uniform gas of density ρ which is calculated with probability$\rho(r)$. Further we can write:

$$\epsilon_{xc}(\rho(r)) = \epsilon_x(\rho(r)) + \epsilon_c(\rho(r)) \tag{5.5}$$

where, ϵ_x is the exchange term, ϵ_c is the correlation term. When the density is not homogenous, LDA is applied by considering homogenous electron gas to be positive. The equation is as follows:

$$\epsilon = -\frac{3}{4}\left(\sqrt[3]{\frac{3}{\Pi}}\right) \int \rho(r^{\frac{4}{3}})\, dr \tag{5.6}$$

The exchange-correlation potential corresponding to the exchange-correlation energy is:

$$V_{xc}(r) = \frac{\delta E_{xc}}{\delta n} \tag{5.7}$$

In LDA, the charge density is non-uniform but the electron gas is uniform and this is the only system for which ϵ_{xc} can be calculated. For electron-rich anions, LDA does not provide accurate description. Hence, LDA predicts erroneously the anionic species to be stable [56].

5.4 Pseudopotential

The electron-ion interaction cannot be accurately described by Fourier components since it decays slowly. Hence, pseudopotential is crucial for plane-wave total energy methods [55]. It represents Columbic potential term for core electrons. Pseudo-wave functions with lesser nodes describe valence electrons. The pseudopotential approximation replaces

core electrons with a weaker potential. It can be represented by Fourier co-efficient. Kohn Sham radial equation which contains the contribution from valence electrons. Softer pseudopotentials have a large cut-off radius but it is less accurate. The use of pseudopotential can help us in reducing the number of electrons, reduce the size of basis sets and include relativistic effects. The most general form of pseudopotential is as follows:

$$NL = \sum lm > V_l < lm \tag{5.8}$$

where, V_l is the pseudopotential for angular momentum, $lm >$ are the spherical harmonics.

A pseudopotential that uses same potential in each angular momentum is called as Local pseudopotential. The drawback of local pseudopotential is that only few elements can be described even if it is computationally much more efficient. In modern plane-wave electronic structure codes, the two most used pseudopotentials are Ultrasoft and Norm-conserving pseudopotentials.

5.4.1 Norm-conserving Pseudopotential

Norm-conserving pseudopotentials are capable of describing the scattering properties of electrons and ions in a variety of atomic environments. It is necessary to have an exchange-correlation defined accurately and, to do so, it is necessary to have the real and pseudo wave functions to be identical so that, from both wave functions, we obtain

identical charge densities. Norm-conserving pseudopotential describes the scattering properties from the ion core.

5.4.2 Ultra-soft Pseudopotential

The ultra-soft pseudopotential was developed by Vanderbilt which is a generalization of the equation of Kleinman-Bylander. This pseudopotential uses fewer plane-waves for calculations and attains smoother pseudo-wave functions. The cutoff energy, when using ultrasoft pseudopotential, is about half that of conventional norm-conserving pseudopotential.

CHAPTER 6

ATOMISTIX TOOLKIT DETAILS

Materials Studio 7.0 was used for carrying out the simulations. It offers a lot of features for materials modeling. There are separate products that integrate into Materials Studio to create a comprehensive range of materials modeling tools. The module used to perform the calculations is CASTEP. The CASTEP module helps to perform first-principles quantum mechanical calculations. This helps to explore the properties of crystals and surfaces in the solid state. The model of graphene structure is verified on the module by establishing a comparison of the literature and experiments. The model is then extended to simulate the properties of graphene.

The performance of CASTEP can be more efficient if the symmetry of the structure is taken into account. Therefore, the symmetry of the structure is considered as P1 symmetry. The time required for a CASTEP calculation increases with the cube of the number of the atoms in the system. The properties that are calculated by using this module are as follows: Band structure of graphene, Density of states, Thermodynamic properties. In calculating the band structures, electronic eigenvalues along high symmetry directions in the Brillouin zone are calculated non-self-consistently for both valence and conduction bands, using electronic charge densities and potentials generated during the simulation. In calculating the density of states, electronic charge densities and potentials are generated during the simulation. In case of phonon dispersion, phonon frequencies and eigenvectors along high symmetry directions in the Brillouin zone are calculated. The results of phonon spectra can be used to compute energy (E), entropy(S), free energy (F) and the lattice heat capacity (C_v) as function of temperature. The results of the

thermodynamic calculations can be visualized using the thermodynamic analysis tools. The formulae are based on the work by Baroni et al. The temperature dependence of the energy is given by:

$$E(T) = E + E_{zp} + \int \frac{\hbar\omega}{\exp\left(\frac{\hbar\omega}{kT}\right)-1} F(\omega)d\omega \quad (6.1)$$

where, E_{zp} is the zero point vibrational energy, k is the Boltzmann constant, $\hbar$ is the Planck's constant, $F(\omega)$ is the phonon density of states. The zero point vibrational energy can be evaluated as follows:

$$E_{zp} = \frac{1}{2}\int F(\omega)\,\hbar\omega d\omega \quad (6.2)$$

The vibrational contribution to the free energy, F, is given by:

$$F(T) = E_{tot} + E_{zp} + kT\int F(\omega)\ln[1-\exp(\frac{\hbar\omega}{kT})]\,d\omega \quad (6.3)$$

The vibrational contribution to the entropy, S, is given as follows:

$$C_v(t) = k\int \frac{\left(\frac{\hbar\omega}{kT}\right)^2 \exp\left(\frac{\hbar\omega}{kT}\right)}{\left[\exp\left(\frac{\hbar\omega}{kT}\right)-1\right]^2} F(\omega)d\omega \quad (6.4)$$

Heat capacity in the Debye model is given by Ashcroft and Mermin. The heat capacity is compared to the actual heat capacity predicted by the Debye model. Hence,

we get the temperature dependent Debye temperature. Heat capacity in Debye model is as follows:

$$C_v{}^D(T) = 9Nk(\frac{T}{\Theta_D})^3 \int \frac{x^4 e^x}{(e^x-1)^2} dx \quad (6.5)$$

where, N is the number of atoms per cell. Thus by calculating the specific heat, we get the actual Debye temperature.

6.1 Molecular Dynamics

Molecular Dynamics is used for calculating the equilibrium statistical-mechanical calculations. Newton's equation is solved step by step from a given starting point. It is implemented by solving DFT equations rather than from empirical potentials of interatomic interactions. With the help of explicit electronic structure optimization, the electrons are kept on the Born-Oppenheimer surface after each step. In CASTEP simulation module, molecular dynamics is based on the Verlet algorithm for integration of the equations of motion.

6.1.1 Ensembles

Newton's equation can help us in exploring the constant-energy surface of the system. When the system is exposed to external pressure, the total energy is not conserved and extended forms of MD is required. Temperature and pressure need to be controlled. The thermodynamic ensembles, handled by CASTEP and the ones which are used, are constant temperature, constant volume (NVT), constant energy, constant volume (NVE).

The system needs to be in thermal equilibrium with minimum energy. Therefore, a system run needs to be done. The ensemble is essential to perform this operation. We have used NVT ensemble to equilibrate the system. It uses Hamiltonian equations of motion. Nose-Hoover thermostat is used. In this thermostat, the position and velocities are generated by adding some dynamic variables which are coupled to the particle velocities. This is called thermostatting.

6.2 Calculation of Phonon Modes

The phonons of a system are calculated by considering a starting point in the force constant matrix. It is given by second derivatives with respect to the atoms in Cartesian space. The force constant matrix between two atoms, i and j, is given by:

$$F(k) = \sum_R \left(\frac{\partial^2 U}{\partial \alpha \partial \beta}\right) \exp(ik(r_{ij} + R)) \tag{6.6}$$

where, R represents the sum over lattice vectors within the cutoff radius. The force constants is then converted into the dynamical matrix D and is given as follows:

$$D_{i\alpha j\beta} = \frac{1}{\sqrt{m_i m_j}} F_{i\alpha j\beta}(k) \tag{6.7}$$

The origin of the three acoustic phonons depends on the energy derivatives. The sum of all the derivatives must be equal to zero when there is no external force. The equation is given as follows:

$$\sum_{i=1}^{N}\left(\frac{\partial U}{\partial \alpha_i}\right) = 0 \tag{6.8}$$

By differentiating the above equation, we get:

$$\left(\frac{\partial^2 U}{\partial \alpha_i \partial \alpha_i}\right) = -\sum r\left(\frac{\partial^2 U}{\partial \alpha_i \partial \alpha_i}\right) \tag{6.9}$$

where, summation excludes the case when i = j. The equation shows that the on diagonal elements of the force constant matrix are equal to the negative sum of the off-diagonal element.

CHAPTER 7

RESULTS AND DISCUSSION

The specific heat of graphene nanoribbon (GNR), both doped and undoped are discussed in this chapter. The simulation shows that the specific heat decreases when the graphene structure is doped with boron and nitrogen. The specific heat of graphene structures has been presented here in Figures 7.1 to 7.5. The specific heat of zig-zag graphene nanoribbon (ZGNR) is as follows:

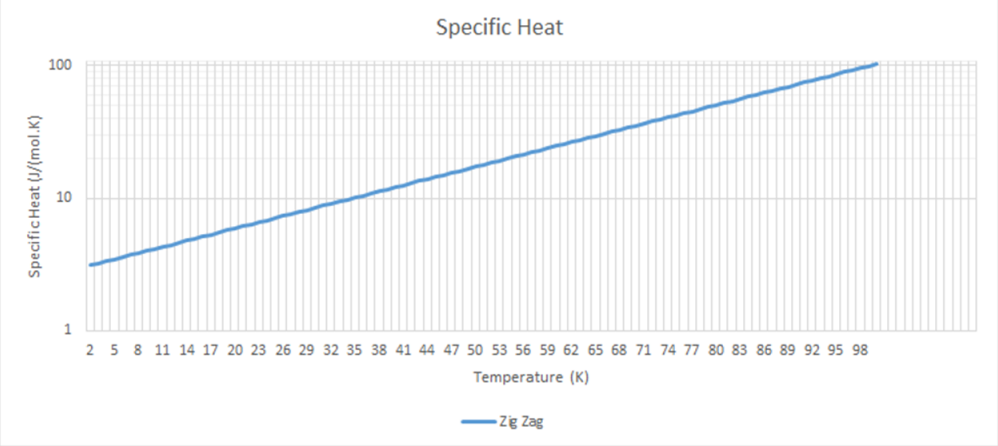

Figure 7.1 Specific heat of zig-zag graphene nanoribbon.

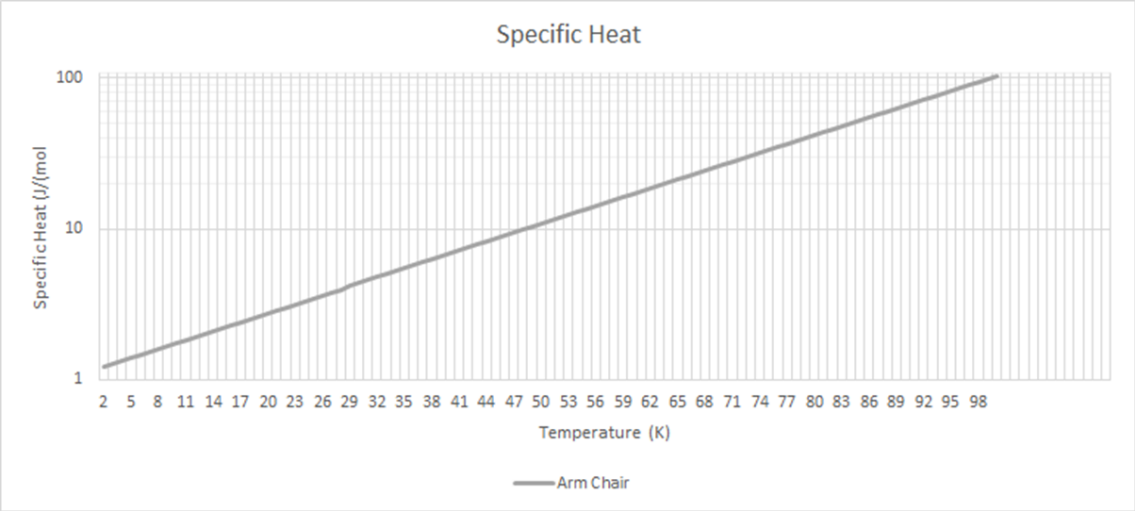

Figure 7.2 Specific heat of armchair zig-zag graphene nanoribbon.

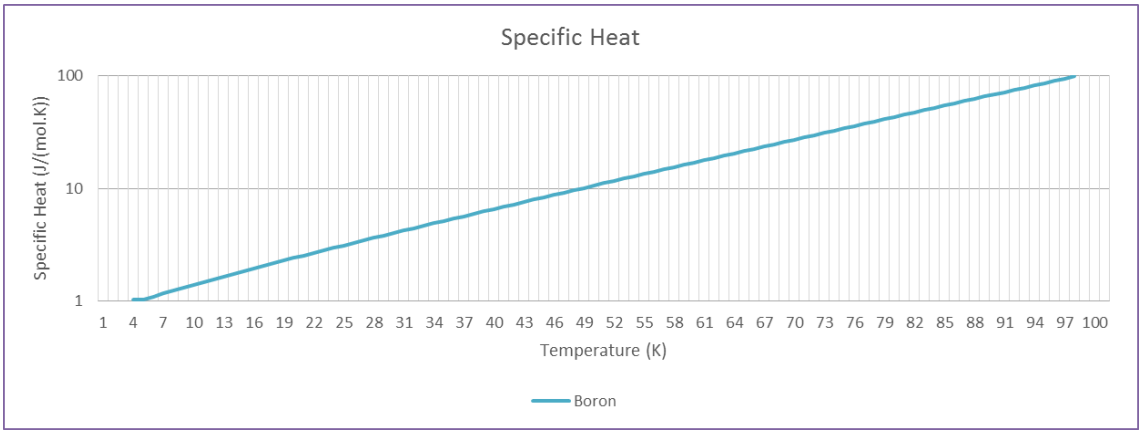

Figure 7.3 Specific Heat of 1% Boron doped graphene nanoribbon.

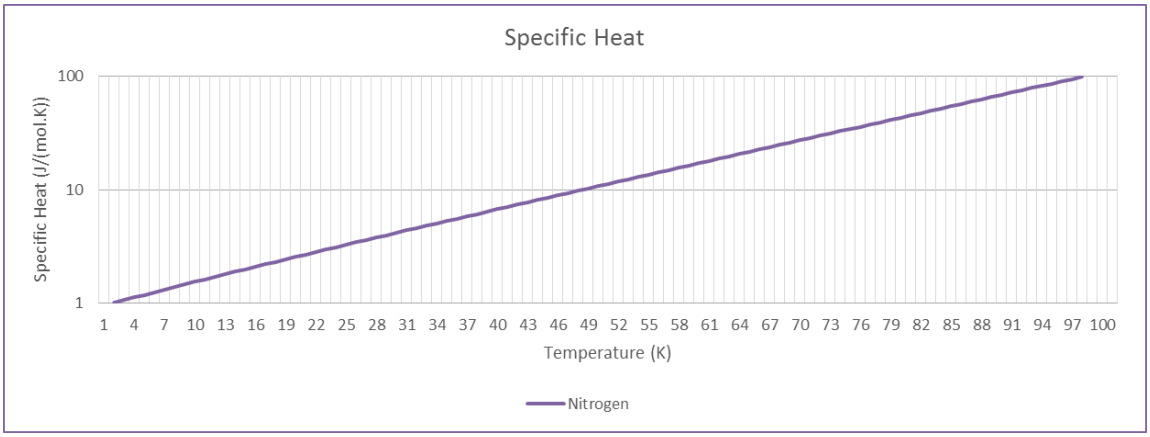

Figure 7.4 Specific heat of 1% Nitrogen doped graphene nanoribbon.

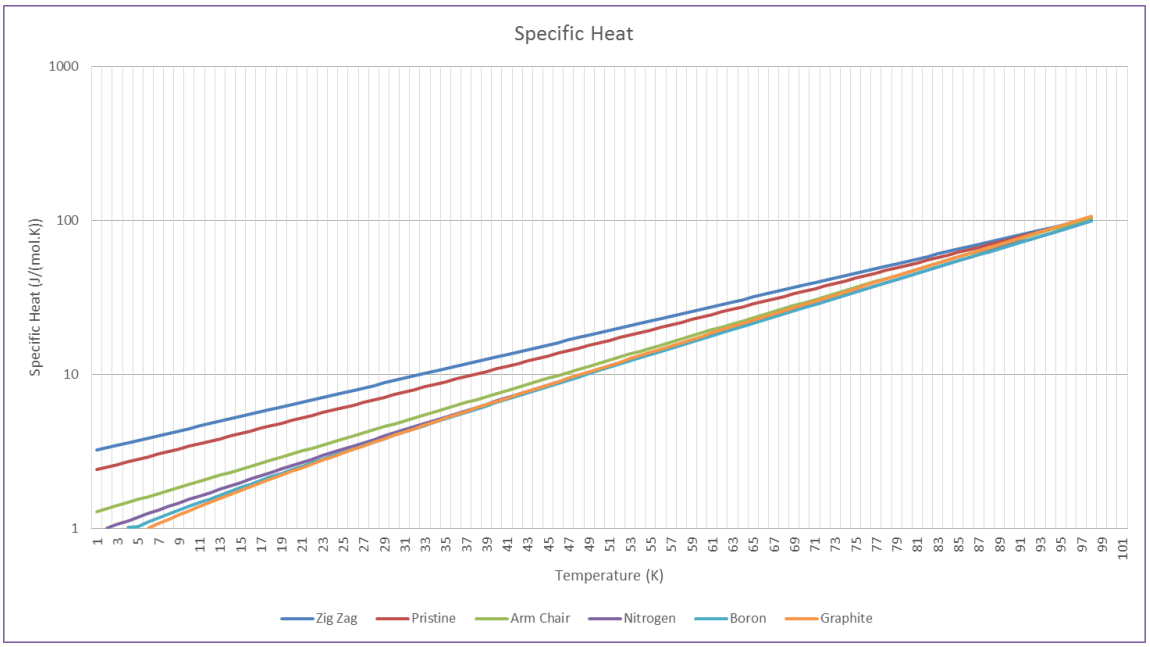

Figure 7.5 Specific heat of various graphene nanoribbons.

Figure 7.5 shows the change in specific heat of various graphene nanoribbons. This is due to increase in phonon scattering which is observed when graphene is doped with boron and nitrogen.

CHAPTER 8

CONCLUSIONS

The materials ability to conduct heat is rooted in its atomic structure. The low-temperature specific heat contains information about both the dimensionality of the system and the phonon dispersion. The specific heat of various graphene structures have been presented. The graphene structures cause phonon quantization which can be observed in the heat capacity at low temperatures. Small quantities of doped nitrogen and boron atoms in graphene structure results in a considerable decline of specific heat of graphene by almost one-half of the ideal sheet.

REFERENCES

1. K. S. Novoselov, A. K. Geim., S. V. Morozov, D. Jiang, Y. Zhang, S. V. Dubonos, I. V. Grigorieva, and A. A. Firsov, *Electric Field Effect in Atomically Thin Carbon Films, Sci.,* (306) (2004), pp. 306-366.

2. A. N. Sidorov, M. M. Yazdanpanah, R. Jalilian, P. J. Ouseph, R. W. Cohn and G. U. Sumanasekera, *Electrostatic deposition of graphene, Nanotech.*, 18 (13) (2007) pp. 135301-135307.

3. K. I. Bolotin, K. J. Sikes, J. Hone, H. L. Stormer and P. Kim, *Temperature Dependent Transport in Suspended Graphene, Phys. Rev. Lett.,* 101 (9) (2008), pp. 096802-096806.

4. H. O. Pierson, (1993), *Handbook of Carbon, Graphite, Diamond and Fullerenes: Properties, Processing and Applications,* (Park Ridge, New Jersey, Noyes Publications).

5. A. K. Geim and K. S. Novoselov, *The rise of graphene, Nat. Materials,* 6 (3) (2007), pp. 183-191.

6. R. W. Cahn and B. Harris, *Newer Forms of Carbon and their Uses, Nat. Materials,* 221 (1969), pp. 132-141.

7. B. Partoens and F. M. Peters, *From graphene to graphite: Electronic Structure around the K point, Phy. Rev. B,* 74 (7) (2006), pp. 075404.

8. M. Ishigami, J. H. Chen, W. G. Cullen, M. S. Fuhrer, and E. D. Williams, *Atomic Structure of Graphene on SiO2, Nano. Lett.,* 7 (6) (2007), pp. 1643-1648.

9. K. S. Novoselov, A. K. Geim, S. V. Morozov, D. Jiang, Y. Zhang, S. V. Dubonos, I. V. Grigorieva and A. A. Firsov, *Electric field effect in atomically thin carbon films Sci.,* 306 (5696) (2004) pp. 666-669.

10. D. Kopeliovich, "*Graphite*" (2013), http://www.substech.com/dokuwiki/doku.php?id=graphite (Accessed 03/26/2015).

11. A. R. Ranjbartoreh, *Advanced mechanical properties of graphene paper, Journal of Appl. Phy.*, 109 (1) (2011), pp. 014306.

12. K. S. Novoselov, A. K. Geim, S. V. Morozov, D. Jiang, Y. Zhang, S. V. Dubonos, I. V. Grigorieva and A. A. Firsov, *Electric field effect in atomically thin carbon films Sci.,* 306 (5696) (2004), pp. 666-669.

13. *"Graphene: Faster, Stronger, Bendier"* (2013), http://www.ft.com/cms/s/0/6f4717b6-66f9-11e2-a83f-00144feab49a.html (Accessed 03/24/2015).

14. Y. Lee, S. Bae, H. Jang, S. Jang, S. Zhu, S. H. Sim, Y. Song, B. H. Hong and J. Ahn, *WaferScale Synthesis and Transfer of Graphene Films, Nano. Lett.,* 10 (2) (2010) pp. 490–493.

15. Q. Yu, J. Lian, S. Siriponglert, H. Li, Y. P. Chen and S. Pei, *Graphene segregated on Ni surfaces and transferred to insulators*, *Appl. Phys. Lett*., 93 (2008), pp. 113103-113106.

16. X. Li, W. Cai, J. An, S. Kim, J. Nah, D. Yang, R. Piner, A. Velamakanni, I. Jung, E. Tutuc, S. K. Banerjee, L. Colombo and R. Ruoff, *Large-area Synthesis of High-Quality and Uniform Graphene Films on Copper Foils*, *Sci.*, 324 (2009), pp. 1312-1314.

17. G. Eda, F. Giovanni and M. Chhowala, *Large-area Ultrathin Films of Reduced Graphene Oxide as a Transparent and Flexible Electronic Material*, *Nat. Nanotech*., 3 (2008), pp. 270-274.

18. D. Wang, Y. Yang, D. Xie, T. Ren and Y. Zhang, *Scalable and Direct Growth of Graphene Micro Ribbons on Dielectric Substrates, Sci. Reports,* (2013), pp. 1348.

19. X. Li, W. Cai, J. An, S. Kim, J. Nah, D. Yang, R. Piner, A. Velamakanni, I. Jung, E. Tutuc, S. K. Banerjee, L. Colombo and R. Ruoff, *Large-area Synthesis of High-Quality and Uniform Graphene Films on Copper Foil*, *Sci*., 324 (2009), pp.1312-1314.

20. A. C. Ferrari, *Raman spectroscopy of graphene and graphite: Disorder, electron–phonon coupling, doping and nonadiabatic effects, Solid State Comm.*, 143 (2007), pp. 47-57.

21. H. Cao, Q. Yu, R. Colby, D. Pandey, C. S. Park, J. Lian, D. Zemlyanov, I. Childres, V. Drachev, E. A. Stach, M. Hussain, H. Li, S. S. Pei and Y. P. J. Chen, *Raman Spectroscopy of Graphene and Related Materials*, *Appl. Phys.*, (2010), pp.044310.

22. "Solid State Physics: Part II Optical Properties of Solids" (2005), http://web.mit.edu/course/6/6.732/www/opt.pdf (Accessed 03/24/2015)

23. A. R. Nistor, D. M. Newns and G. J. Martyna, *The role of chemistry in graphene doping for carbon-based electronics*, *ACS Nano.*, 5 (3096) (2011).

24. Y. Z. Yu, Y. Zhao, S. Ryu, L. E. Brus, K. S. Kim, P. Kim, *Tuning the Graphene Work Function by Electric Field Effect, Nano. Lett*., 9 (10) (2009), pp. 3430-3434.

25. X. Wang, X. Li, L. Zhang, Y. Yoon, P. K. Weber, H. Wang, J. Guo and H. Dai, *N-doping of graphene through electro thermal reactions with ammonia, Sci.,* 324 (2009), pp. 768.

26. Z. S. Wu, W. Ren, L. Xu, F. Li and H. M. Cheng, *Doped graphene sheets as anode materials with super high rate and large capacity for lithium ion batteries, ACS Nano.,* 5 (2011), pp. 5463.

27. S. Park and R. S. Ruoff, *Chemical methods for the production of graphenes, Nat. Nanotech.*, 4 (2009), pp. 217-224.

28. G. Jo, M. Choe, S. Lee, W. Park, H. Y. Kahng and T. Lee, *The application of graphene as electrodes in electrical and optical devices, IOP Sci., Nanotech.,* 23 (11) (2012).

29. T. Borca-Tasciuc, D. Achimov, W. L. Liu and G. Chen, *Thermal conductivity of InAs/AlSb superlattices*, 5 (2000), pp. 369-372.

30. A. K. Geim and K. S. Novoselov, *The rise of graphene, Nat. Materials*, 6 (2007), pp. 183–191.

31. H. O. Pierson, (1993), *Handbook of Carbon, Graphite, Diamond and Fullerenes: Properties, Processing and Applications,* (Park Ridge, New Jersey, Noyes Publications).

32. A. A. Balandin, *Thermal properties of graphene and nano structured carbon materials, Nat. Materials*, 10 (2011), pp. 569-581.

33. C. Y. Ho, R. W. Powell and P. E. Liley, *Thermal conductivity of the elements: a comprehensive review, J. Phys. Chem. Ref. Data*, 1 (2) (1972).

34. J. M. Ziman, *Electrons and Phonons: The Theory of Transport Phenomena in Solids, Sci.,* 133 (3447) (2009), pp. 187-188.

35. J. E. Parrott and A. D. Stuckes, *Thermal Conductivity of Solids,* (1975), pp. 143-150.

36. J. Zou, A. Balandin, *Phonon heat conduction in a semiconductor nanowires, J. Appl. Phy.*, 89 (1959), pp. 2932.

37. P. G. Klemens, *Advances in research and applications, Solid State Phy.*, 7 (1958), pp. 1-98.

38. G. Basile, C. Bernardin and S. Olla, *Momentum conversion model with anomalous thermal conductivity in low dimensional system*, *Phys. Rev. Lett.*, 96 (2006), pp. 204303-204304.

39. D. L. Nika, N. D. Zincenco and E. P. Pokatilov, *Engineering of Thermal Fluxes in Phonon Mismatched Heterostructures, J. Nanoelect. Optoelect.*, 4 (2009), pp.180.

40. J. M. Ziman: *Electrons and Phonons: The Theory of Transport Phenomena in Solids* (Oxford University Press, 2001).

41. P. G. Klemens, *Thermal Conductivity and Lattice Vibrational Modes Solid State Physics, Adv. Res. Appl.*, 7 (1958).

42. E. Pop, V. Vashney and A. K. Roy, *Thermal Properties of graphene: Fundamentals and applications*, 37 (2012), pp. 1273-1281.

43. T. Tohei, A. Kuwabara, F. Oba and I. Tanaka, *Debye temperature and stiffness of carbon and boron nitride polymorphs from first principles calculations*, *Phys. Rev. B*, 73 (2006), pp. 064304.

44. L.X. Benedict, S.G. Louie and M.L. Cohen, *Solid State Comm.*, 100 (1996), pp. 177.

45. T. Tohei, A. Kuwabara, F. Oba, I. Tanaka, *Debye temperature and stiffness of carbon and boron nitride polymorphs from first principles calculations*, *Phys. Rev. B*, 73 (2006), pp. 064304.

46. J. Hone, *Phonons and Thermal properties of Carbon Nanotubes*, *Springer-Verlag*, (2001), pp. 273-280.

47. V. N. Popov, *Low-temperature specific heat of nanotube systems*, *Phys. Rev. B*, 66 (2002), pp. 153408.

48. L. E. Fried, W. E. Howard, *Explicit Gibbs free energy equation of state applied to the carbon phase diagram*, *Phys. Rev.*, 61 (2000) pp. 8734.

49. S. Chen, Q. Wu, C. Mishra, J. Kang, H. Zhang, K. Cho, W. Cai, A. A. Balandin and A. S. Ruoff, *Thermal conductivity of isotopically modified graphene*, *Nat. Materials*, 11 (2012), pp. 203.

50. S. Stackhouse, *Theoretical Methods for Calculating the Lattice Thermal Conductivity of Minerals*, 71 (2010), pp. 253-269.

51. H. Adachi, T. Mukoyama and J. Kawai: *Hartree-Fock-Slater Method for Materials Science: The DV-X Alpha Method for Design and Characterization of Materials.* (Springer International Publishing, 2006).

52. P. Hohenberg and W. Kohn, *Inhomogeneous Electron Gas*, *Phy. Rev*., 136 (3B) (1964), pp. B864-B871.

53. S. Kotochigova, Z. H. Levine, E. L. Shirley, M. D. Stiles and C. W. Clark, (NIST: Physical Measurement Laboratory, NIST, 2014).

54. W. Kohn and L. J. Sham, *Self-Consistent Equations Including Exchange and Correlation Effects, Phy. Rev.,* 140 (4A) (1965), pp. A1133-A1138.

55. S. Narasimhan, *"The Self Consistent Field (SCF) loop and some Relevant Parameters for Quantum –ESPRESSO"*, 2221 (5) (2011).

56. J. P. Perdew and A. Zunger, *Self-interaction correction to density-functional approximations for many-electron systems, Phy. Rev. B,* 23 (10) (1981), pp. 5048-5079.